Int. J. Nanosci. Nanotechnol., Vol. 9, No. 2, June 2013, pp. 61-70

Irradiation with Neutrons and Formation of Simple Radiation Defects in Semiconductors

Sh. Sohrabnezhad[1*], D. Rezaei Ochbelgh[2], N. Morsali Golboos[2]

1- Department of Chemistry, Faculty of Science, University of Guilan, Rasht, I. R. Iran
2- Department of Chemistry, Faculty of Science, University o f Mohaghegh Ardabili, Ardabil, I. R. Iran

(*) Corresponding author: sohrabnezhad@guilan.ac.ir
(Received:10 Feb. 2013 and Accepted: 23 June 2013)

Abstract:
In this research, cobalt and nickel sulfide nanoparticles (NPs) were grown on AlMCM-41 matrix by using ion exchange method. The prepared samples were irradiated by thermalized neutron that emitted from Am-Be source up to fluencies (7.9+E9n/cm^2). After that, X-ray diffraction (XRD), UV-Vis spectroscopy, Fourier transform infrared (FTIR), scanning electron microscopy (SEM) and transmission electron microscopy (TEM) were used for irradiated and non-irradiated samples characterization. The results show nanoparticles aggregation in NiS/AlMCM-41 is more than CoS/AlMCM-41 sample. The TEM images show average size of CoS NPs before and after neutron radiation about 20 and 50 nm, respectively. In this way, average size of NiS nanoparticles before and after neutron radiation 130 and 70 nm respectively. The DRS results show that Co^{2+} and Ni^{2+} ions produced after neutron radiation, located in tetrahedral sites in AlMCM-41. The results indicate host materials have important role in decrease of radiation defects (RDs).
Keywords: *Nanocomposite, Neutron Irradiation, Diffuse Reflectance Spectroscopy, Aggregation, Radiation Defects.*

1. INTRODUCTION

One of the attractive research fields in recent years is synthesis of various sizes and shapes of semiconductor materials nanoparticels. The goal of these activities is improving the performance and utilization of nanoparticles in various applications from sensing devices to photonic materials in molecular electronics and to advanced oxidation techniques (AOTs). The size and shape dependent optical and electronic properties of these nanoparticles make an interesting case for exploiting them in light induced chemical reaction [1].

The main drawbacks are the need for complex filtration procedures and the high turbidity that decreases the radiation flux. Such problems have motivated the development of supported photocatalysts in which semiconductors is immobilized on different adsorbent materials. In this contest, molecular sieves have attracted greater attention due to their adsorption capacity that helps in pooling the pollutants to the vicinity of the semiconductors surface [2-4]. Molecular sieves offer excellent control of size distribution and morphology through the main pulsation of the wet chemical processing parameters. Microporous molecular sieves have been widely used for hosting nanoparticles, but they are limited to pore opening of less than 1nm [5]. The recent discovery of mesoporous MCM-41 offers a possibility for

synthesizing 3D heterostructures in a previously inaccessible size range, by inclusion chemistry [6]. MCM-41 is a porous amorphous silica material with a hexagonal honeycomb structure that can be synthesized with controllable pore diameter in the range 2-10 nm. However, incorporation of aluminum into the structure of MCM-41materials via isomorphous substitution of aluminum for silicon, generate ion exchange sites in this mesoporous molecular sieves [7]. Therefore, cationic metals such as Co^{2+} or Ni^{2+} can be incorporated into AlMCM-41 by ion exchange method [8, 9].

One of the principal causes of radiation damage to electronic devices is due to neutron. Because neutrons are relatively heavy (1840 times heavier than electrons) uncharged particles, instead of merely ionizing atoms or molecules, they collide with the lattice atoms of the semiconductor, displacing whole atoms from their lattice sites to cause them take up interstitial positions within the crystal. This results in disruption or distortion of the local lattice structure [10].

A number of articles have been published on investigating radiation defects (RDs) in semiconductors. In particular, the influence of different types of radiation including electrons, ions and neutrons on semiconductor properties were studied [11, 12]. It was shown that irradiation with electrons of E<5 MeV energy at room temperature gives rise to the formation of simple RDs in semiconductor. But the irradiation with neutrons, protons and higher energy electrons produce more complex RDs. The RDs essentially influence electrical, optical and structural properties of the devices manufactured on its base.

The aim of this work is study of optical properties CoS and NiS semiconductor in AlMCM-41 host material under the influence of thermal neutrons radiation. The study was carried out in room temperature. CoS/AlMCM-41 and NiS/AlMCM-412 nanocomposite were prepared by ion exchange method.

To investigate neutron effects in nano-composites, we described below some results that obtained from high-tech instruments such as XRD (X-ray Diffraction), SEM (Scanning Electron Microscopy), transmission electron microscopy (TEM), UV-Vis spectroscopy and FT-IR (Fourier transform infrared) for irradiated and non-irradiated samples. The results show that irradiation with neutron at room temperature formed simple RDs in semiconductors incorporated in AlMCM-41.

2. EXPERIMENTAL

2.1. Synthesis of AlMCM-41 material

The MCM-41 and AlMCM-41 materials were synthesized by a room temperature method with some modification in the described procedure in the literature [13]. We used tetraethylorthosilicate (TEOS: Merck,800658) as a source of silicon and Hexadecyltrimethylammonium bromide (HDTMABr;BOH,103912) as a surfactant template for preparation of the mesoporous material. The molar composition of the reactant mixture is as follows:

SiO_2:1.6EA:0.215HDTMABr:325H O: 0.1Al_2O_3

Where the EA stands for ethylamine. The MCM-41 prepared was calcined at 550˚C for 5h to decompose the surfactant to obtained white powder. This powder was used as the parent material to prepare AlMCM-41 free surfactant materials by ion-exchange method with 0.1 M of $Al_2(SO_4)_3.18H_2O$ (Merck) solution. AlMCM-41 surfactant-free was used for loading the nanoparticles.

2.2. Preparation of CoS/MCM-41and NiS/MCM-41 catalysts

The 0.1 M solution of $CoCl_2$ and $NiCl_2$ was prepared as precursors of the CoS and NiS semiconductors. For ion-exchange, 1 gr of AlMCM-41 powder was separately suspended in 50 ml solution of $CoCl_2$ and $NiCl_2$ and stirred at room temperature for 5h. After that, the samples were washed to remove unexchanged ions and then air-dried.

Finally, sulfurizing of ions was carried out with 0.1 M Na_2S solution. To make the reaction with the S^{-2} ion, 0.5 gr of Co^{+2} and Ni^{2+} exchanged mesopore samples separately were added to 50 ml of 0.1 M Na_2S solution at a fixed temperature and magnetically stirred for 5h. The Samples were washed with deionized water and collected by

filtration. The obtained samples were fine powders with grey color. The prepared samples are called CoS/AlMCM-41 and NiS/AlMCM-41.

2.3. Irradiation

Obtained powder samples were divided into two parts. One of them was kept as reference specimen and the other was irradiated for 16h by Am-Be neutron source (with a 5.2 Ci activity) that surrounded by PE (Polyethylene) with a thickness of 5cm. Figure 1 illustrates setup that assembled to irradiated specimen by neuron source. The Am-Be neutron source that used to irradiate specimen has an activity 5.2 Ci. The neutron radiation fluencies used is about 7.9E+9n/cm^2.

Figure 2 shows spectrum of neutron energy for this type of neutron source [12]. As seen in Figure 2, most of emitted neutrons have high energy. In general, fast neutrons (E> 10KeV) are required to convert on low energy neutrons As seen in Figure 3, because of low cross section, fast neutron cannot interact with Co and S. In the research to obtain low energy neutrons a thickness of 5cm PE used to surround neutron source (Figure 1).

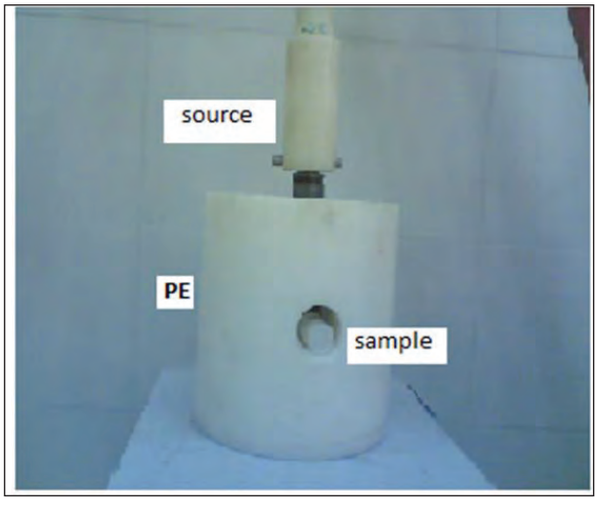

Figure 1: *Photograph of experimental setup to irradiate samples by neutron source.*

2.4. Characterization

Powder X-ray diffraction patterns of the samples were recorded using an X-ray diffractometer (Bruker D8 Advance) with Co Kα radiation (λ=1.789A˚) under the conditions of 40 KV and 30 mA, at a step size of 2Θ=0.02˚. The UV–Vis diffused reflectance spectra (UV–vis DRS) obtained from UV–vis Scinco 4100 spectrometer with an Integrating sphere reflectance accessory.

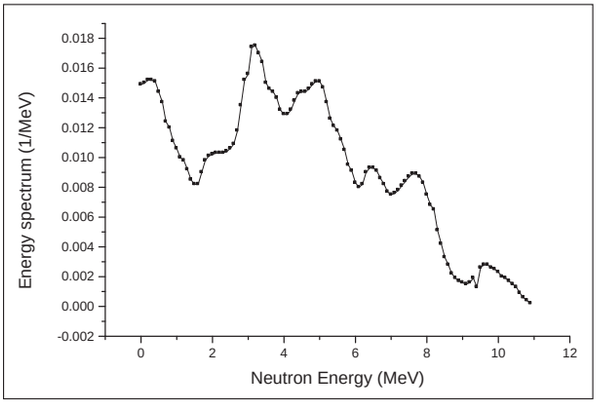

Figure 2: *Typical Neutron energy spectrum for Am-Be neutron source.*

$BaSO_4$ Was used as reference material UV–Vis absorption spectra were recorded using a Shimadzu 1600 PC in the spectral range of 190-900 nm. The surface morphology of the samples was obtained using a Loel-1430 VP scanning electron microscopy and finally infrared spectra on KBr pellet were measured on a Bruek spectrophotometer. The transmission electron micrographys (TEM) were recorded with a Philips CM10 microscope, working at a 100 kV accelerating voltage. Samples for TEM were prepared by dispersing the powdered sample in acetone by sonication and then drip drying on a copper grid coated with carbon film.

3. RESULTS AND DISCUSSION

3.1. XRD results

The XRD pattern of AlMCM-41 support, non-irradiated and irradiated CoS/AlMCM-41 and NiS/AlMCM-41 is show in Figure 4. The XRD pattern of AlMCM-41 show typical characteristic three-peak pattern with a very strong one at a low 2θ and two peaks at higher 2θ values [14, 15]. The

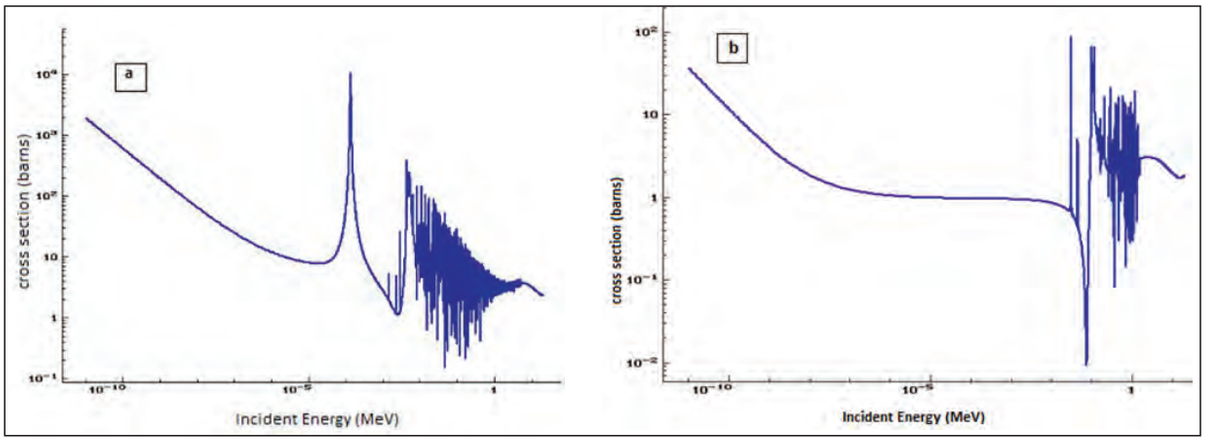

Figure 3: *Neutron cross section variations via neutron energy for (a) Co and (b) S.*

XRD patterns of non-irradiated samples are similar AlMCM-41 sample. But, some differences, such as the broadening of the diffraction peaks, increasing or decreasing of some peaks intensity as well as the shift of the peak position to lower angles can be observed in the spectra. For example increasing the range from 2θ = 2-10º to 2θ = 2-80º shows only one broad (100) peak at 2θ = 2.2º for non-irradiated NiS/AlMCM-41 sample (insert Figure 4a). However, with limiting the range to 2θ = 25-45º, in irradiated samples, two peaks are observed (Figure 4b) approximately at 2θ equal 30º and 55º, which are due to the reflection of the ~30º (100) and ~53º (110) planes, in the nanoNiS phase, respectively [16,17]. Proceeding in the same way, we found one peak in the case of CoS, at 29º (100) which is related to the (100) plane of CoS phase [17].

3.2. UV-Vis spectra

UV-visible absorption spectra for irradiation and non-irradiation samples are given in Figure 2. The diffuse reflectance spectra for irradiate sample NiS/AlMCM-41 show absorption band at wavelengths of 657, 594 and 489 nm. In the same way, CoS/AlMCM-41 sample show absorption band at wavelengths of 620, 552 and 492 nm. These bands belong to tetrahedral Ni^{2+} and Co^{2+} ions in mesoporous materials, respectively [18, 19]. In fact, NiS and CoS particles are turned to Ni^{2+} and Co^{2+} ions by neutron radiation. Neutron radiation directly interacts with nuclei and releases free- radicals. Released radical's causes to accomplish chemical bindings between particles and so, produce ions.

3.3. FT-IR spectra

The FT-IR spectra nanoparticles of CoS/AlMCM-41 and NiS/AlMCM-41 samples for irradiated and non-irradiated are shown in Figure 6 and Figure 7, respectively. The FT-IR samples show similar bands. But, some differences such as increasing or decreasing of some bands intensity as well as the shift of peak position to the slightly lower angles can be observed in the spectra. These can be attributed to interaction of Co^{2+} ions or Ni^{2+} ions with AlMCM-41 material. In fact, chemical binding for semiconductors was broken by neutron radiation [19, 20]. Then change in absorbance can not be related to degradation of host material during neutron irradiation because the FT-IR spectra nanoparticles of samples for irradiated and non-irradiated are similar.

3.4. SEM images

Figure 8 shows SEM images of irradiated and non-irradiated samples. As seen in Figure 8 large aggregation is observed in non-irradiated NiS/MCM-41sample. But it is lower in irradiated sample. Therefore, It is clear that when neutron radiation interact with NiS/MCM-41 sample decrease aggregation. As seen in Figure 8 large aggregation is observed in irradiated CoS/MCM-41 sample. But

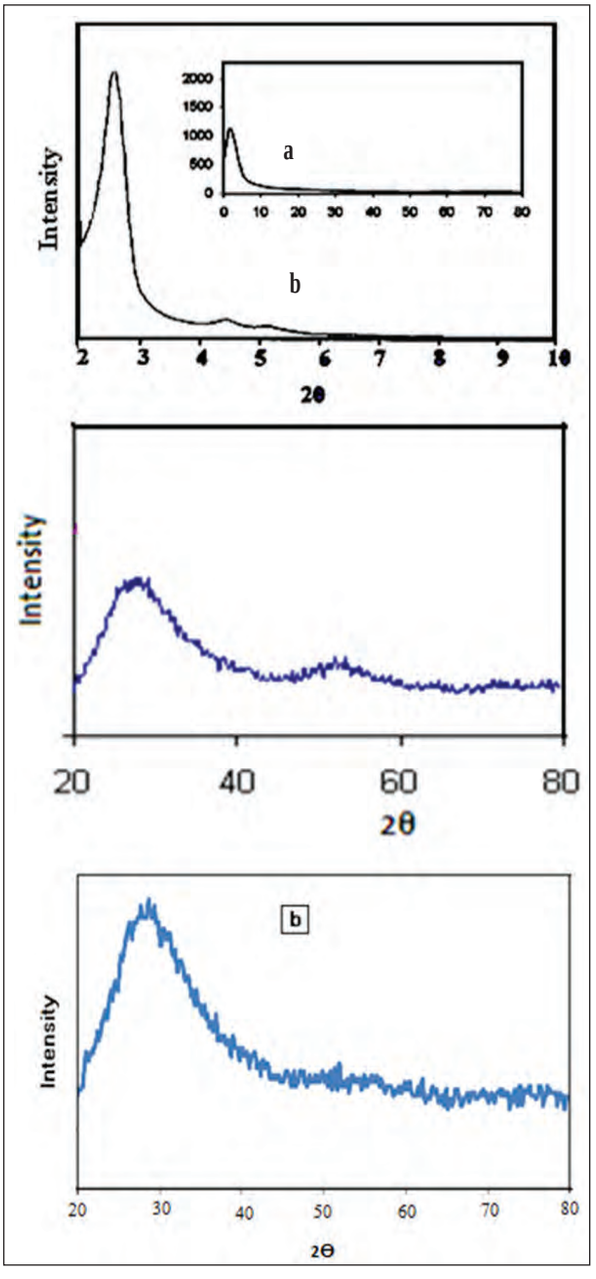

Figure 4: *X-ray diffractograms of (a) AlMCM-41 (b) irradiated © (c) irradiated CoS/AlMCM-41. The insert shows XRD pattern of the non-irradiated ©.*

it is lower in non-irradiated sample. Therefore, It is clear that when neutron radiation interact with CoS/MCM-41 sample increase aggregation. Neutron radiation interacts with target nuclei without any restriction. Neutron radiation directly interacts with

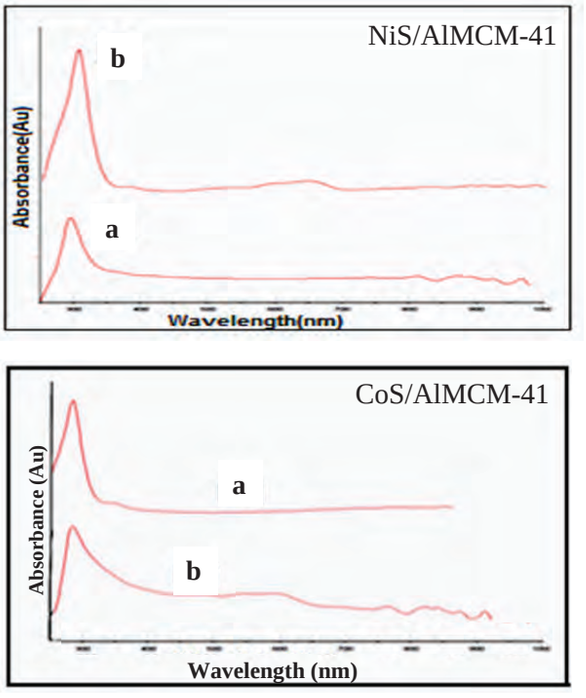

Figure 5: *Absorption spectra of samples (a) non-irradiated and (b) neutron irradiated samples.*

nuclei and releases free-radicals. Released radical's causes to accomplish chemical bindings between particles and so, increase aggregation in remainder CoS nanoparticles.

3.5. TEM images

TEM images of samples are shown in Figure 9. Even darker images have been obtained on AlMCM-41 reference indicating that the dark aspect can be associated with the presence of water trapped inside AlMCM-41 grains [21]. The particle size of AlMCM-41 and non-irradiate sample of CoS/AlMCM-41observed from TEM photographs is around 20 nm (Figure 9 a, b) and no change in the particle size of AlMCM-41 is observed on modification with CoS nanoparticles. The particle size in irradiated sample (Figure 9c) is more than non-irradiated sample (50 nm). In the way, particles size NiS before and after irradiated is 130 and 70 nm, respectively (Figure 9 d, e). Neutron radiation directly interacts with nuclei and releases free-

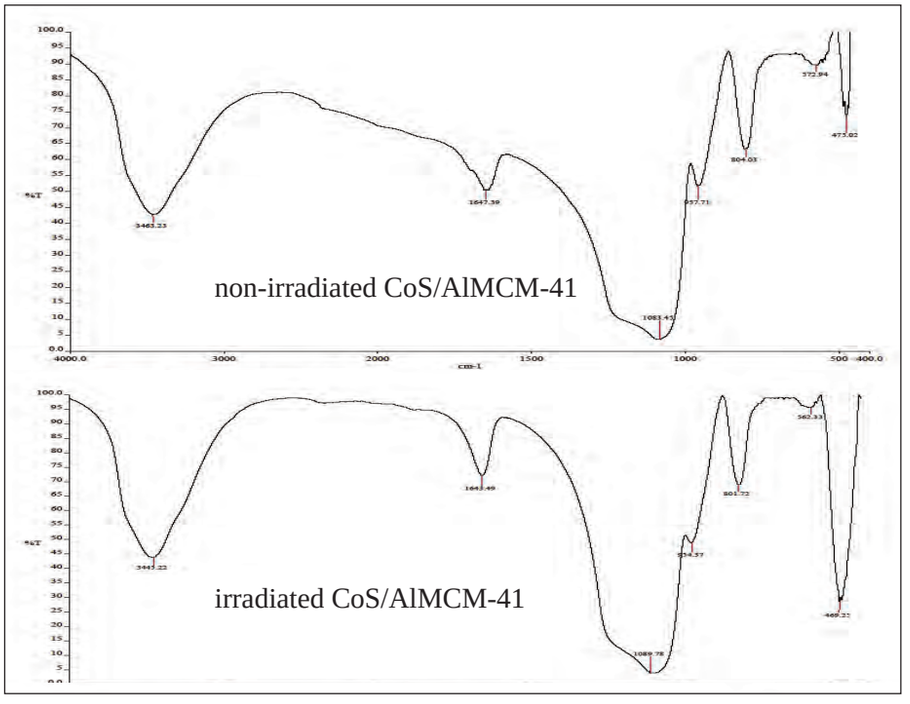

Figure 6: *FT-IR spectra of samples (CoS/AlMCM-41)*

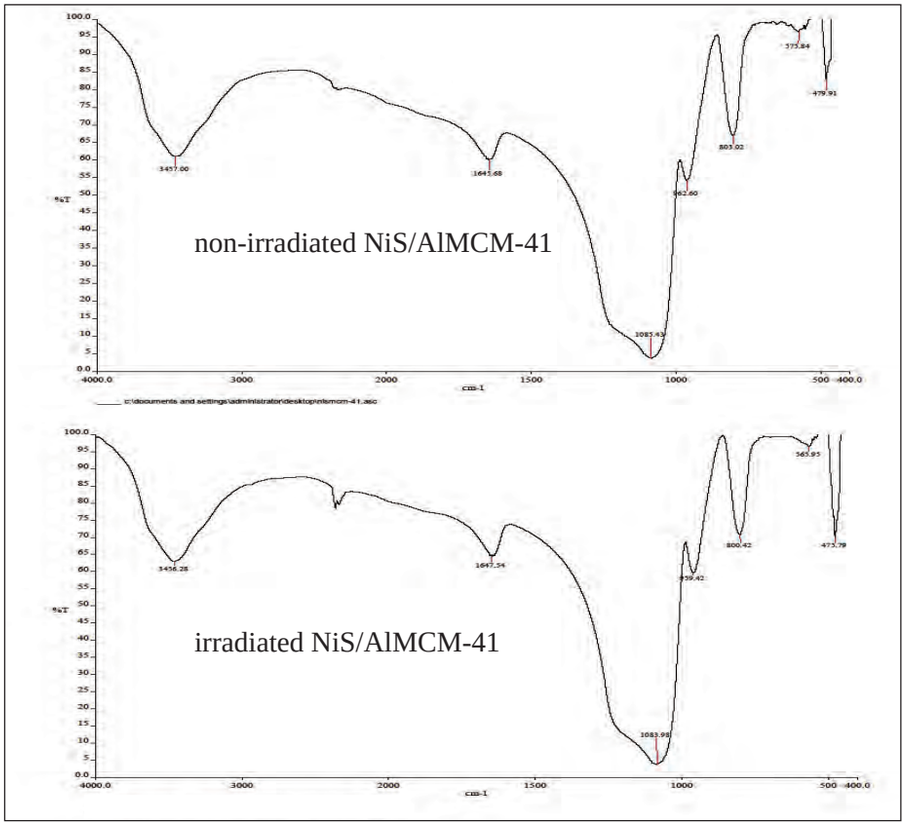

Figure 7: *FT-IR spectra of samples (NiS/AlMCM-41)*

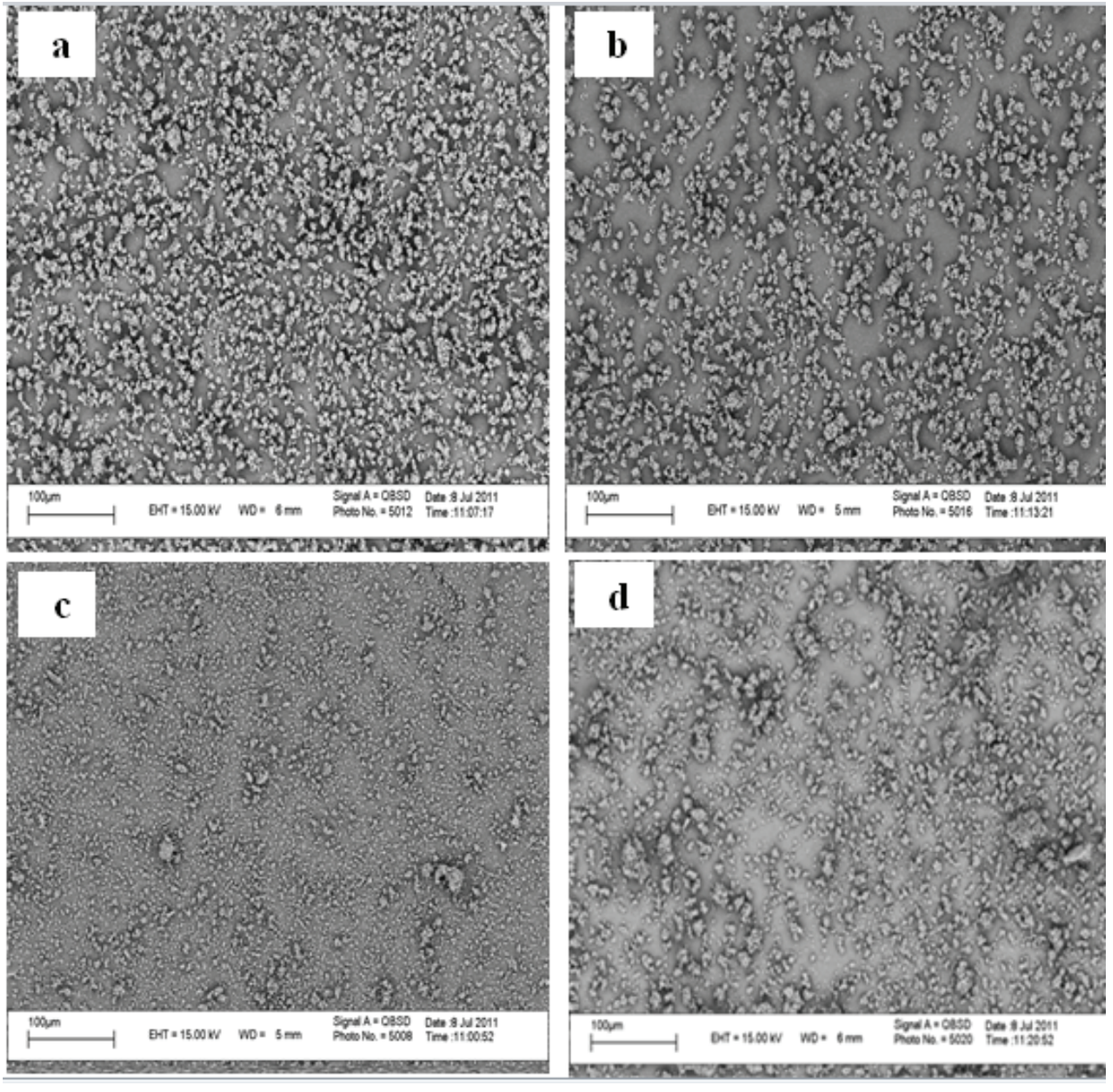

Figure 8: *Scanning electron micrographs of (a) non-irradiated NiS/AlMCM-41and (b) irradiated NiS/AlMCM-41 (c) non-irradiated CoS/AlMCM-41 (d) irradiated CoS/AlMCM-41samples.*

radicals. Released radical's causes to accomplish chemical bindings between nanoparticles and so, increase aggregation in remainder nanoparticles. Meanwhile, there is not change in morphology of host material.

4. CONCLUSIONS

In this work, CoS and NiS nanoparticles are prepared in AlMCM-41 by ion exchange method. Neutron radiation interacts with target nuclei without any

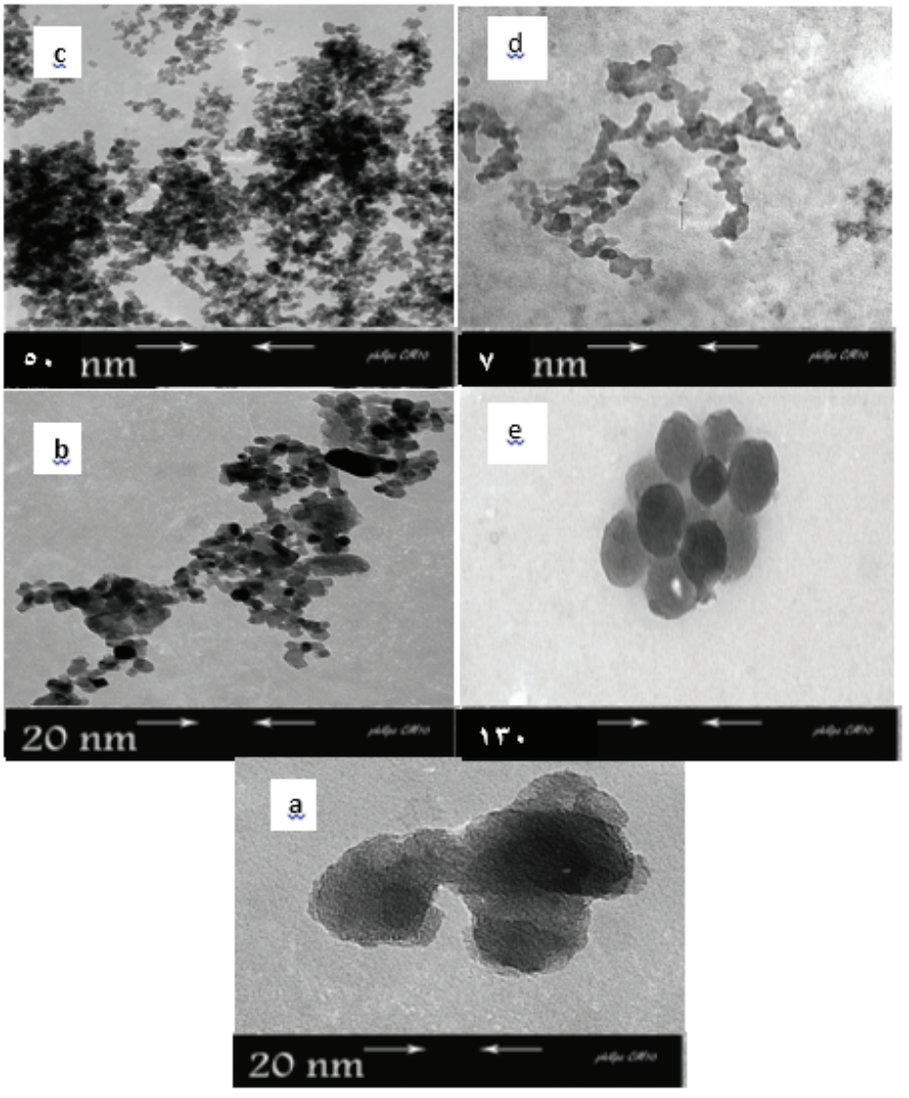

Figure 9: *TEM Images of (a) Host material, (b) non-irradiated CoS/AlMCM-41 and (c) irradiated CoS/AlMCM-41 (d) irradiated NiS/AlMCM-41 (e) non-irradiated NiS/AlMCM-41 samples.*

restriction. Neutron radiation directly interacts with nuclei and releases free-radicals.

Released radical's causes to accomplish chemical bindings between particles and so, increases and degreases aggregation in remainder CoS and NiS nanoparticles, respectively. In facts, irradiation with neutron at room temperature formed simple RDs in nanocomposite semiconductors incorporated in AlMCM-41. Change in optical properties can not be related to degradation of host material based on spectra images and hosting material has important role in causing simple radiation defect by semiconductor neutron interaction.

REFERENCES

1. Sh. Sohrabnezhad, A. Pourahmad, E. Radaee, Photocatalytic degradation of basic blue 9 by CoS nanoparticles supported on AlMCM-41 material as a catalyst, J. Hazard. Mater. Vol. 170 (2009), pp. 184-190.

2. W. Panpa, P. Sujarid Worakan, S. Jinawath, Photocatalytic activity of TiO_2/ZSM-5 composites in the presence of SO_4^{2-} ion, Applied Catalysis B: Environmental. Vol. 80, (2008), pp. 271-276.

3. V. Druga Kumari, M. Subrahmanyam, K.V. Subbax Rao, A. Ratnamala, M. Noorjahan, K. Tanaka, An easy and efficient use of TiO_2 supported HZSM-5 and TiO_2 + HZSM-5 zeolite combinate in the photodegradation of aqueous phenol and p-chlorophenol,_Appl. Catal. A: Gen. Vol. 234, (2002), pp. 155-165.

4. M. V. Shankar, S. Anandan, N. Venkatachalam, B. Arabindoo, V. Murugesan, Fine route for an efficient removal of 2,4-dichlorophenoxyacetic acid (2,4-D) by zeolite-supported TiO_2, Chemosphere, Vol. 63, (2006), pp. 1014-1021.

5. G. Schulz-Ekloff, D. Wöhrle, B. van Duffel, and R. A. Schoonheydt, Chromophores in porous silicas and minerals: preparation and optical properties, Micropor. Mesopor. Mater. Vol. 51, (2002), pp. 91-138.

6. L.Z. Zhang, P. Cheng, G – Q. Tang, D - Z. Liao, Electronic properties of an organic molecule within MCM-41host: a spectroscopic and theoretical study toward elucidating the variation in band gaps of the guest species, Journal of Luminescence, Vol. 104, (2003), pp. 123-129.

7. D. Wei, H. Wang, X. Feng, W. Chuch, P. Ravikovitch, M. Lyubovsky, C. Li, T. Tekeguchi, G.L. Holler, Synthesis and Characterization of Vanadium-Substituted Mesoporous Molecular Sieves, J. Phys. Chem. B Vol. 103, (1999), pp. 2113-2121.

8. A. Pourahmad, Sh. Sohrabnezhad. E. Radaee, Degradation of basic blue 9 dye by CoS/ nanoAlMCM-41 catalyst under visible light irradiation, J. Porous. Mater, Vol. 17, (2010), pp. 367-375.

9. Sh. Sohrabnezhad, A. Pourahmad, As-synthesis of nanostructure AgCl/Ag/MCM-41 composite, Spectrochim. Acta A, Vol. 86, (2012), pp. 271-275.

10. A. A. Haider F, Ch. Abdulah, Neutron radiation effects on metal oxide semiconductor (MOS) devices, Nucl. Instrum. Methods Phys. Res., sect. B, Vol. 267, (2009), pp. 3032-3036.

11. N.G. Kolin, D.I. Merkurisov, S.P. Solov,ev. Radiation effects on the electrical activation processes in InSb under influence of nuclear reactor neutrons, Physica B, Vol. 307, (2001), pp. 258-264.

12. K. Takakura, K. Hayama, D. Watanabe, H. Ohyama, T. Kudou, K. Shigaki, S. Matsuda, S. kuboyama, T. Kishikawa, J. Uemura, E. Simoen, C. Claeys, An improvement of electrical characteristics of P-N diode by X-ray irradiation method Physica B, Vol. 376-377, (2006), pp. 403-406.

13. A.C. Voegtlin, A. Matijasic, J. Patarin, C. Saucrland, Y. Griller, L. Huve, Microporous Mater. Vol. 10, (1997), pp. 137-147.

14. Q. Cai, Z.-Sh. Luo, W.Q. Pang, Y.-W. Fan, Xi–H. Chen, F.-Zh. Cui, Dilute solution routes to various controllable morphologies of MCM-41 silica with a basic medium, Chem. Mater. Vol. 13, (2001), pp. 258–263.

15. M.-Ch. Chao, H.-P. Lin, Ch.-Y. Mou, Bo.-W. Cheng, Ch.-F. Cheng, Synthesis of nano-sized mesoporous silicas with metal incorporation, Catal. Today, Vol. 4, (2004), pp. 81–87.

16. A. Pourahmad, Sh. Sohrabnezhad, Synthesis and characterization of CoS nanoparticles encapsulated in mesoporous aluminosilicate material by solid-state reaction, Mater. Lett. Vol. 65, (2011), pp. 205-207.

17. Q. Wang, Zh. Xu, H. Yin, Q. Ne, Synthesis of copper sulfide nanotube in the hydrogel system, Mater. Chem. Phys. Vol. 90, (2005), pp. 73–77.

18. R.A. schoonheydt, D. Roodhooft and H. Leeman, Coordination of Ni^{2+} to lattice oxygens of the zeolites X and Y, Zeolites. Vol. 7, (1987), pp. 412-417.

19. A. A Verberckmoes, B. M. Weckhuysen, R. A. Schoonheydt, Spectroscopy and Coordination Chemistry of Cobalt in Molecular Sieves, Micropor. Mesopor. Mater. Vol. 22, (1998), pp. 165-178.

20. J. Janas, T. Shishido , M. Che, S. Dzwigaj, Role of tetrahedral Co(II) sites of CoSiBEA zeolite in the selective catalytic reduction of NO: XRD, UV–vis, XAS and catalysis study, Appl. Catal., B, Vol. 89, (2009), pp. 196-203.

21. J. K. Reddy, V. Durgakumari, M. Subrahmanyan, B. Sreedhar, Anwendung von porosem Glas als Tragermaterial in der Ubergangsmetallkatalyse Mater. Res. Bull. Vol. 44, (2009), pp. 1540-1546.